



# University of HUDDERSFIELD

## University of Huddersfield Repository

Palmer, Edward and Fieldhouse, John D.

Comparison of air flow and heat dissipation from the front brakes fitted to a high performance GT Car

### Original Citation

Palmer, Edward and Fieldhouse, John D. (2007) Comparison of air flow and heat dissipation from the front brakes fitted to a high performance GT Car. In: Proceedings of Computing and Engineering Annual Researchers' Conference 2007: CEARC'07. University of Huddersfield, Huddersfield, pp. 1-8.

This version is available at <http://eprints.hud.ac.uk/3702/>

The University Repository is a digital collection of the research output of the University, available on Open Access. Copyright and Moral Rights for the items on this site are retained by the individual author and/or other copyright owners. Users may access full items free of charge; copies of full text items generally can be reproduced, displayed or performed and given to third parties in any format or medium for personal research or study, educational or not-for-profit purposes without prior permission or charge, provided:

- The authors, title and full bibliographic details is credited in any copy;
- A hyperlink and/or URL is included for the original metadata page; and
- The content is not changed in any way.

For more information, including our policy and submission procedure, please contact the Repository Team at: [E.mailbox@hud.ac.uk](mailto:E.mailbox@hud.ac.uk).

<http://eprints.hud.ac.uk/>

# COMPARISON OF AIR FLOW AND HEAT DISSIPATION FROM THE FRONT BRAKES FITTED TO A HIGH PERFORMANCE GT CAR

E Palmer, R. Mishra and J. Fieldhouse  
University of Huddersfield, Queensgate, Huddersfield HD1 3DH, UK

## ABSTRACT

Within this paper the convective heat dissipation from the front brake discs fitted to the left and right hand side of a high performance passenger car has been compared. The tools used in this investigation include computational fluid dynamics (CFD) and vehicle testing. The results show that although identical discs are fitted to both sides of the vehicle the disc fitted to the left hand side shows better thermo-aerodynamic properties than that fitted to the right due to the different direction of rotation. The computational model shows strong agreement with the test results; over predicting the average heat transfer coefficient by 4% for the left hand disc and 7.6% for the right disc. The CFD analysis enabled a detailed insight into the air flow and heat transfer distributions that was not possible during the vehicle test regime.

**Keywords** CFD, Brake Cooling, Heat transfer

## 1 INTRODUCTION

The increased refinement of passenger vehicles has caused the expectations of the consumer to rise. This has put considerable pressure on the automotive industry to produce ever quieter cars, none more so than in the area of brake refinement. Of the classifications of brake noise, judder is now regarded as the most concerning of all brake problems, accounting for 75% of brake refinement issues [1]. This translates to a cost to the industry of \$100 million (US) a year in warranty claims alone, so the magnitude of this problem is evident [2]. In order to prevent the occurrence of judder as well as many other forms of brake noise, excessive heating of the brake disc must be avoided, whilst minimizing temperature variations across the rotor. This is in direct contradiction with the additional demands placed on the braking system by the increasing vehicle weight and engine performance. This is especially prevalent within the luxury grand touring market; where the highest levels of performance and refinement are expected by the customer.

It is clear that to increase a brake rotors resistance to producing noise and fade, it must be designed such that it ensures sufficient uniform heat dissipation and thermal capacity [3]. In high demand braking applications vented discs consisting of two rubbing surfaces separated by straight radial vanes are normally employed as they utilise a greater surface area to dissipate heat.

In this paper the airflow through and convective heat dissipation from the front brake discs of a high performance grand touring passenger car has been investigated using a computational fluid dynamics (CFD) code. The quantitative results obtained from the computational analysis are validated with data obtained in high speed vehicle testing at Millbrook test facility. The focus of this work is the comparison of the disc fitted to the left and right hand sides of the car. The design of the brake disc features 40 vanes with an initial inlet angle of  $0^\circ$ . Then at approximately 60% of the disc radius the vane angle changes by  $30^\circ$ . Identical discs are fitted to the left and right hand side of the car, causing them to rotate in opposite directions to one another.

## 2 EXPERIMENTAL METHODOLOGY

An essential part of any computational analysis is validation against a data set which is both repeatable and accurate. Within the field of automotive braking there are two main sources of data for validation; the brake dynamometer and vehicle testing. The brake dynamometer does not offer a true picture of the aerodynamic performance of the brake rotor due to the vast differences in the surrounding geometry of the disc which is known to have a large effect on disc performance [4]. Therefore it is necessary to perform vehicle testing in order to quantify the differences between dynamometer testing, computational analysis and real world application.

The vehicle test procedure was devised to replicate the power inputs of a manufacturer's standard judder performance test within the restraints of testing in the UK. The test consists of 19 high speed, low deceleration braking events to condition the brakes for judder. High speed stops are used in order to quickly dissipate a large amount of heat energy into the brake system therefore giving the potential for large thermal gradients within the rotor. This large input of energy into the brake rotor provides the ideal conditions for the thermo-elastic deformations that can lead to the occurrence of judder. Low deceleration rates of 0.2-0.4g are utilised in order to prevent pressure from the braking system 'ironing out' deformations in the rotor and maximising the chances of the vehicle occupants to experience the symptoms of judder.

The vehicle testing equipment included:

- Embedded thermocouples positioned half across the face of both the inner and outer rubbing surfaces of the front brake rotors, connected via slip rings provided an accurate measurement of the disc surface temperatures, see figure 1.
- A rubbing thermocouple mounted on the left hand rear brake rotor provided a reference temperature.
- Two axis accelerometers mounted on the brake caliper and inner brake pad back plate provided information on the tangential and axial vibrations.
- High frequency pressure transducers to measure fluctuations in the brake fluid pressure, allowing fluctuations caused by disc thickness variations to be analyzed.
- Vehicle speed was provided via a GPS system.
- Vehicle deceleration was measured with an accelerometer fitted within the cabin.
- Pedal effect and travel were measured with load and displacement transducers.
- A modular data logging system capable of recording the 19 channels of data required in real-time.
- A laptop to enable real-time viewing of brake temperature, vehicle speed and vehicle deceleration. This increased the repeatability of the test procedure and reduced the level of experimental error.

### 3 EXPERIMENTAL RESULTS

CFD employs mathematical models to simulate a physical flow field. This includes a set of partial differential equations and boundary conditions. The CFD package used in this study is the commercially available code *Fluent 6.0*. *Fluent* solves Navier-stokes equations along with the continuity equations and appropriate auxiliary equations depending on the type of applications using a control volume formulation. In the present case the conservation equations for mass, momentum and energy have been solved with two additional flow transport equations for steady turbulent flow.

The equation for conservation of mass given below is valid for both incompressible and compressible flows. The source term  $S_m$  is the mass added to the continuous phase from the dispersed second phase (e.g. Due to vaporization of liquid droplets) and any user defined sources.

$$\frac{\partial \rho}{\partial t} + \nabla \cdot (\rho \vec{v}) = S_m \quad (1)$$

Conservation of momentum in the  $i^{\text{th}}$  direction in an inertial (non accelerating) reference frame is given by

$$\frac{\partial (\rho \bar{u}_i)}{\partial t} + \nabla \cdot (\rho \bar{v}_i \vec{v}) = -\nabla p + \nabla \cdot (\bar{\tau}_i) + \rho \bar{g}_i + \bar{F}_i \quad (2)$$

The stress tensor is given by

$$\tau_{ij} = \mu [(\nabla \vec{v} + \nabla \vec{v}^T) - \frac{2}{3} \nabla \cdot \vec{v} I] \quad (3)$$

Where  $\mu$  is the molecular viscosity,  $I$  is the unit tensor, and the second term on the right hand side is the effect of volume dilation.

To model the flow of energy fluent employs the equation for energy which is given in the vector form by

$$\frac{\partial}{\partial t}(\rho E) + \nabla \cdot (\vec{v}(\rho E + p)) = \nabla \cdot (k_{eff} \nabla T - \sum_j h_j \vec{J}_j + (\vec{\tau}_{eff} \cdot \vec{v})) + S_h \quad (4)$$

$k_{eff}$  is the effective conductivity ( $k + k_t$ , where  $k_t$  is the turbulent thermal conductivity, defined according to the turbulence model being used), and  $\vec{J}_j$  is the diffusion flux of species  $j$ . The first three terms on the right-hand side of the equation represent energy transfer due to conduction, species diffusion, and viscous dissipation, respectively.  $S_h$  includes the heat of chemical reaction [4].

Fluent uses the finite volume method to solve the Navier-Stokes equations and is known for its robustness in simulating many fluid dynamic phenomena. The finite volume method consists of three stages; the formal integration of the governing equations of the fluid flow over all the (finite) control volumes of the solution domain. Then discretisation, involving the substitution of a variety of finite-difference-type approximations for the terms in the integrated equation representing flow processes such as convection, diffusion and sources. This converts the integral equation into a system of algebraic equations, which can then be solved using iterative methods [5]. The first stage of the process, the control volume integration, is the step that distinguishes the finite volume method from other CFD methods. The statements resulting from this step express the 'exact' conservation of the relevant properties for each finite cell volume. This gives a clear relationship between the numerical analogue and the principle governing the flow.

To enable the modeling of a rotating body (in this case the disc) the rotating reference frame technique is employed. This technique utilizes modified versions of the momentum and conservation equations. In terms of absolute velocities the left hand side of the momentum equations becomes

$$\frac{\partial}{\partial t}(\rho \vec{v}) + \nabla \cdot (\rho \vec{v}_r \vec{v}) + \rho(\vec{\Omega} \times \vec{v}) \quad (5)$$

$\vec{v}_r$  is defined as relative velocity and  $\vec{\Omega}$  is the angular velocity vector. The continuity equation employed in rotating reference frame problems is written as:

$$\frac{\partial \rho}{\partial t} + \nabla \cdot (\rho \vec{v}_r) = S_m \quad (6)$$

The test data relating to disc temperature, ambient temperature and vehicle speed was used to provide vital information for the generation of accurate boundary conditions such as rotor surface temperature as well as speed of rotation. Implementation of boundary conditions that accurately replicate the real braking events is fundamental if the comparison of results is to be meaningful. The disc was modeled as a shell rotating in still air; implementing atmospheric pressure and temperature at the inlet and outlet boundaries. The atmospheric temperature was taken to be 14.72°C, corresponding to vehicle test data. The walls of the disc are represented as smooth walls with a uniform temperature of 500°C. Symmetrical boundary conditions have been used to generate zero-shear slip walls at the edge of the domain [4]. A 9 degree segment of the rotor (equating to one vane) was modeled using the periodic boundary conditions, as described above. This had the effect of making the model much smaller, translating to lower hardware requirements and saving vast amounts of computational time. The speed of rotation for the simulation of the left hand disc is 1140rpm and -1140rpm for the right hand disc. This corresponds to the test vehicle speed that correlates to a rotor temperature of 500°C. This is taken from the cooling period after the stops, as this is the closest to steady state conditions achieved during testing. In the present analysis flow is assumed to be turbulent as the Reynolds numbers of the flow is found be greater than  $10^5$  over the first row of pins. The Reynolds number is calculated from the inlet velocity obtained using equations proposed by Limpert [6]. To model the turbulence the semi-empirical K- $\epsilon$  turbulence RNG model is employed in this study as it was found to give stronger convergence than the standard K- $\epsilon$  model. A complete summary of the boundary conditions used is given in figure 2.

Through the use of a mesh independence analysis and volume mesh optimization using a fine mesh near the walls of the disc and coarse mesh near the boundaries of the domain, the variation in results was found to become insignificant with approximately 1.3 million tetrahedral elements.

## 4 EXPERIMENTAL RESULTS

The data from the final set of follow-on stops (stops 14-19) is displayed in figure 2. This period of test represents the highest disc temperatures and levels of energy saturation within the brake system. The average temperature of the inner and outer rubbing surfaces for both the left and right hand rotors is presented along with the vehicle speed.

As well as providing information for accurate boundary conditions (as described above) the test data is also able to provide the information on the heat transfer characteristics of the rotor. The heat transfer rate and heat transfer coefficient have been calculated from the first derivative of temperature with respect to time. Taking the average temperature of the inner and outer rubbing surfaces yields a heat transfer rate of 27.5KW and an average heat transfer coefficient of 104.5W/m<sup>2</sup>K for the left hand disc at a temperature of 500°C and rotational speed of 1140rpm. With the same conditions the right hand disc the heat transfer rate of the right hand disc is 14.4% lower at 24.3KW, equating to a heat transfer coefficient of 89.5 W/m<sup>2</sup>K.

The left hand disc reaches a maximum temperature of 635.1°C at the end of the 19<sup>th</sup> stop. The maximum temperature achieved by the right hand disc was 12.7°C higher than the left at 647.8°C. This temperature difference can be partially accounted for by the different thermal cycles created by braking on a banked high speed test track. It can also be attributed to the 11.6% lower heat transfer rate from the right hand disc, as this makes it less efficient at dissipating energy which leads to higher temperatures.

## 5 COMPUTATIONAL RESULTS

The relative velocity magnitude at 50% of channel height (taken at channel exit) is depicted in figure 4. As with the static pressure distribution it can be seen that the flow field velocity magnitudes within both brake discs vary over a broad range. Within the left hand brake disc there are regions of high velocity at the entrance to the channel and along the trailing edge of the vane, with a maximum velocity of 24.9m/s occurring at radius ratio 0.63 and non-dimensional channel width of 0.1. This figure also shows regions of low velocity occurring between radius ratio 0.7 and 1.1 on the leading edge of the vane where the relative velocity ranges from 8.3m/s to approximately 15m/s and region of separation at ratio 0.97 and channel width of 0.9 on the trailing edge of the vane at the channel exit.

There is a negligible change in the range of values of velocity magnitude between the left and right hand disc but there is a significant change in the velocity distribution. As with the left hand brake disc; a region of high velocity can be seen at the vane passage entrance (radius ratio 0.63) on the rotor fitted to the right hand side of the car. However the maximum velocity of 27.2m/s occurs on the trailing edge of the vane at the passage exit (radius ratio 0.97). As can be seen with the left rotor the right hand disc has a region of low velocity between radius ratio 0.7 and 1. The region forms on the trailing edge of the vane and is substantially larger than that seen in the left hand disc with lower velocities.

Figure 5 depicts the three dimensional path lines through the discs fitted to both the left and right hand side of the vehicle. The flow pattern through the left hand disc shows the formation of vortices at the inlet generated by the flow over the vane trailing edge. The flow separates from the leading edge of the vane at a radius ratio of 0.7. However unlike many straight radial vane vented rotors [8] areas of recirculation are avoided, as the separated flow joins the vortices generated at the inlet. This results in a positive radial velocity distribution across the width and length of the vane passage giving the rotor a high pumping efficiency. The flow pattern through the disc fitted to the right hand side of the car however shows a distinct region of separation. The flow separates from the trailing edge of the vanes at a radius ratio of 0.7 and does not reattach before the passage exit. This generates a region of recirculation characterized by negative radial velocities next to the trailing edge of the vane, reducing the pumping efficiency of the disc.

To quantify the effects of the above flow parameters on the thermo-aerodynamic properties of the rotor the mass flow rate of air passing through the discs has been computed. The mass flow rate through the model of the left hand rotor was found to be 0.0145Kg/s equating to a mass flow rate through a complete rotor of 0.58Kg/s. The mass flow rate through the right hand disc model was computed to be 0.0101Kg/s equating to a mass flow rate through the entire disc of 0.404Kg/s. When comparing the left and right hand discs this represents a 30% decrease in the overall mass flow rate from the left to right hand rotors.

Figure 6 depicts the static temperature distributions on a plane at 50% of channel height (taken at channel exit) within the left and right hand brake discs. A comparison of figures 5 and 7 shows that in both discs the regions of lower velocity magnitude correspond with the regions of elevated temperature. In the case of the left hand brake rotor the region of maximum velocity magnitude corresponds to the minimum temperature of 300.1K, the maximum temperature of 618K occurred in the region of low velocity at the exit of the channel. With the right hand disc it can be clearly seen that there is a larger region of higher temperatures, corresponding with the larger region of lower velocity seen in figure 5. The maximum temperature obtained is 764.9K in the region of recirculation on the trailing edge of the vane (at radius ratio 0.8). The minimum temperature is located at the inlet of the vane passage; however another region of low temperature is apparent at the location of maximum velocity.

Contours of heat transfer coefficient extracted from CFD analysis for both rotors are presented in figure 7. The distribution of heat transfer coefficient over the rotors surface is highly non-uniform, with troughs in the low velocity regions and peaks in high velocity regions. This is because high energy dissipation occurs in high velocity regions and low energy dissipation in low velocity regions. The heat transfer coefficient values for the left hand rotor vary from approximately 50W/Km<sup>2</sup> to 325.1W/Km<sup>2</sup>, resulting in an average heat transfer coefficient of 108.9W/Km<sup>2</sup> over the entire rotor, equating to a heat transfer rate of 28.53KW for the entire disc. Regions of high heat transfer can be seen at the passage inlet and along the trailing edge of the vane, corresponding to the regions of high velocity and low temperature in figures 5 and 7. Regions of low heat transfer coefficient occur on the outer rubbing surfaces of the disc where the minimum heat transfer coefficient is seen. An area of low heat transfer, also seen on the leading edge of the vane, form a radius ratio of 0.7, corresponding to the area of low velocity and high temperature presented in figure 5 and 7 respectively.

The range of values for the heat transfer coefficient across the surface of the right hand rotor was calculated to be approximately 30W/Km<sup>2</sup> to 304.9W/Km<sup>2</sup>. This results in an average heat transfer coefficient of 96.8W/Km<sup>2</sup>; this generates a heat transfer rate of 26.29KW. As with the left hand disc the region of highest heat transfer occurs at the inlet to the passage with region of poor heat transfer on the rubbing surfaces of the rotor. A region of poor heat transfer also occurs on the walls of the passage next to the region of recirculation.

## 6 CONCLUSION

The results presented show that the brake rotor studied generally has very good thermo-aerodynamic properties. When fitted to the left hand side of the car the disc avoids many of the aerodynamic problems associated with rotors of this type, such as separation and recirculation. However when fitted to the right hand side of the vehicle some of these problems become apparent. In vehicle testing this resulted in an 11.6% decrease in the heat transfer from the rotor. This result was repeated in the CFD analysis which saw a 7.85% decrease from the disc fitted to left to the right of the vehicle. The insight enabled by the CFD analysis shows that the decrease in heat transfer can be attributed to the reduced mass flow rate through the rotor passage caused by the increase in separation and the subsequent regions of recirculation.

There is very good correlation between the computational model and the experimental data: The CFD model of the left hand rotor over predicted the heat transfer coefficient and heat transfer rate by 4% The right hand model over predicts the heat transfer rate and heat transfer coefficient by 7.6%. This can be attributed to the simplification is the geometry surrounding the rotor; in the model the disc rotates in open air ignoring the effect of the wheel or arch geometry which is known to have a large effect on the aerodynamic characteristics of the disc [7]. Without these features to obstruct the flow the mass flow rate through the disc will be higher than when the rotor is in situ, generating higher heat transfer.

## REFERENCES

Thompson J, *State of the Art towards the NVH Robust Brake – USA Position Brakes 2006*, An NVH Robust Brake Session, 07/05/2006

Akebono Braking Technology, *Brake Noise, Vibration and Harshness: Technology Driving Customer Satisfaction*, Akebonobrakes.com, 2005

Dahm K L & Dearnley P A, *Thermal Modelling of Disc Brake Rotors to Enable the Optimal Exploitation of Surface Engineering* IMechE, Brakes 2006 pp 115-124, 2006

Sisson A, *Thermal Analysis of Vented Brake Rotors* SAE paper No.780352, 1978  
Fluent Inc. *Fluent User Guide* Fluent Inc. 2003

H K Versteeg & W Malalasekera, *An Introduction to Computational Fluid Mechanics; The Finite Volume Method* Prentice Hall, 1995

Limpert R, "Cooling Analysis of Disc Brake Rotors" SAE Paper 751014, 1975

Kubota M., Hamabet, NakazonoY, Fukuda M., Doi K. (2000), *Development of a Lightweight Brake Disc Rotor: A Design Approach for Achieving an Optimum Thermal, Vibration and Weight Balance*. JSAE paper No. 2000-497-502



Figure 1: Thermocouple in Front Brake Disc and Test Vehicle Fitted with Slip Rings

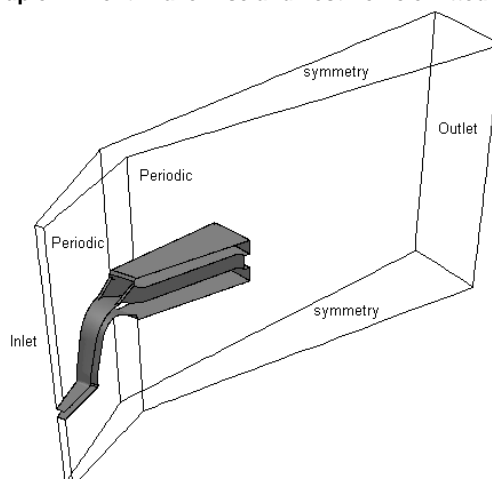


Figure 2: CFD Boundary Conditions

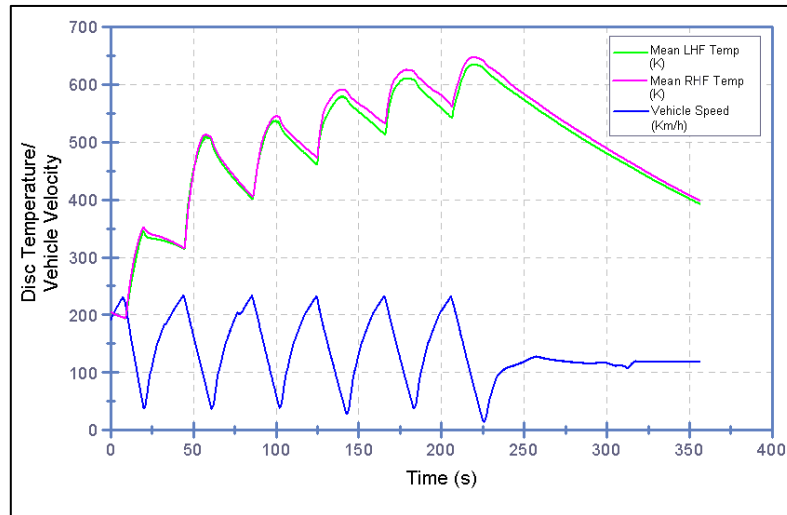


Figure 3: Experimental Results

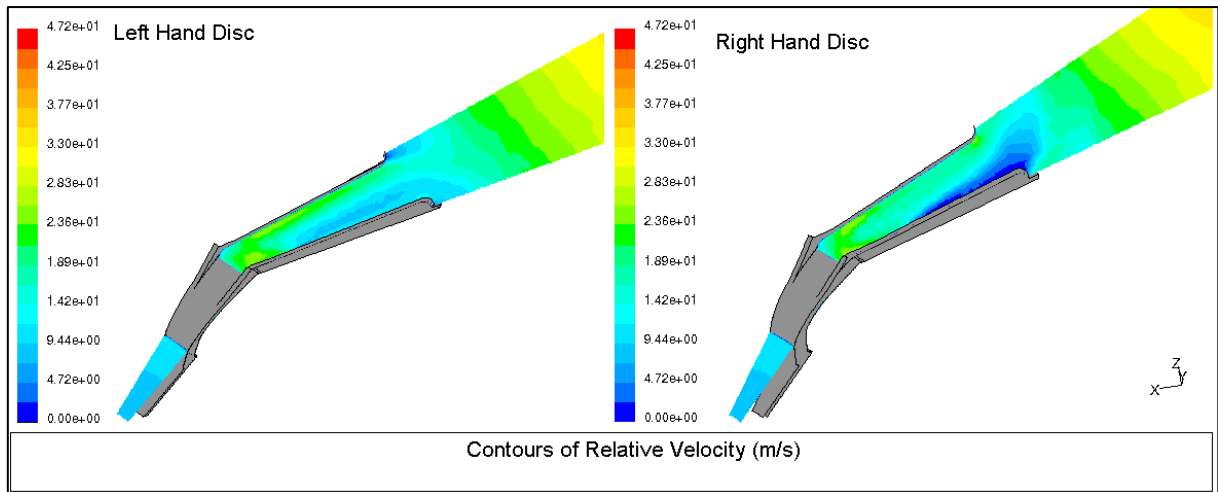


Figure 4: Relative Velocity Distribution

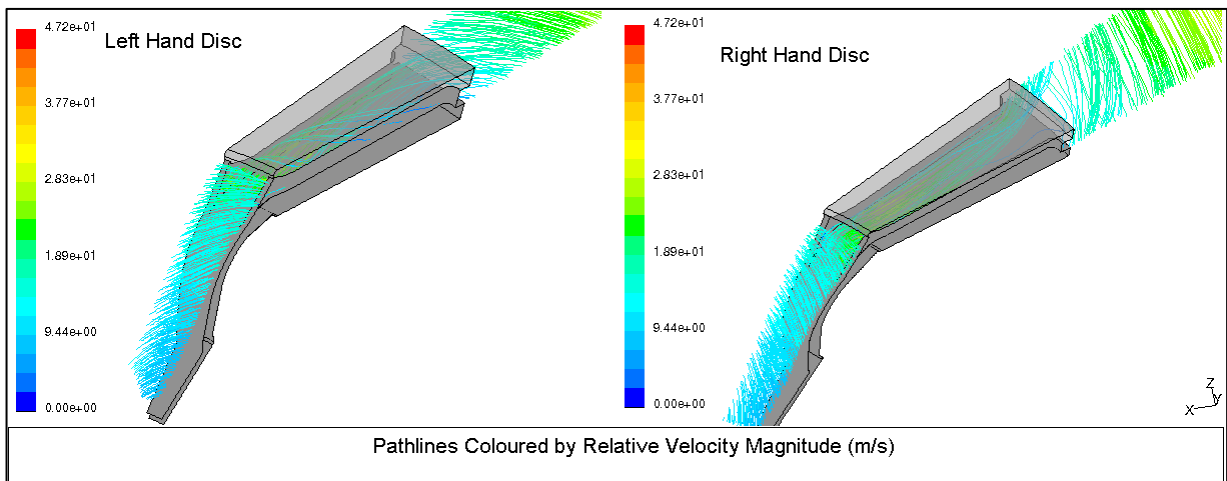


Figure 5: Path lines

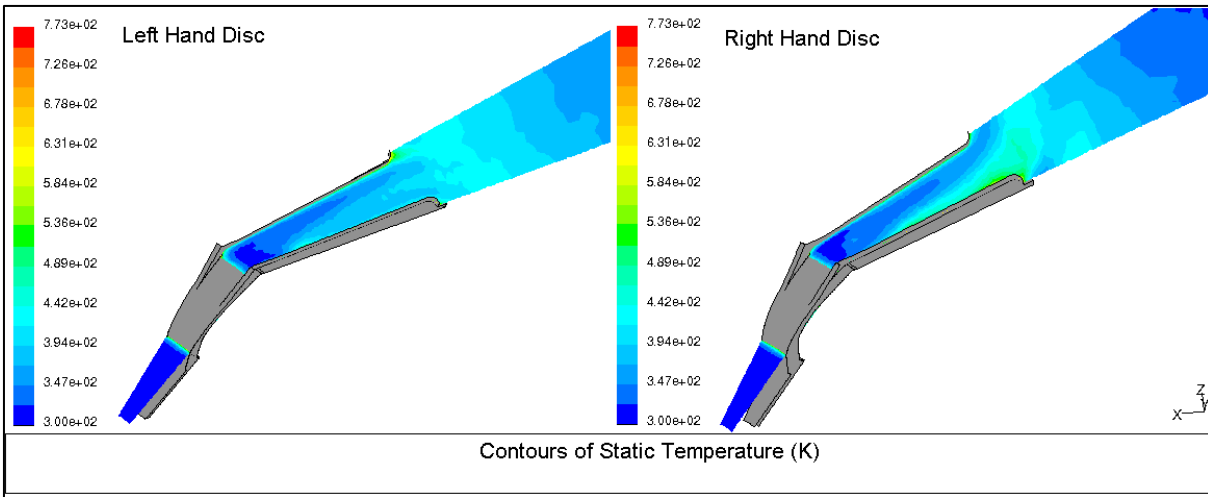


Figure 6: Temperature Distributions

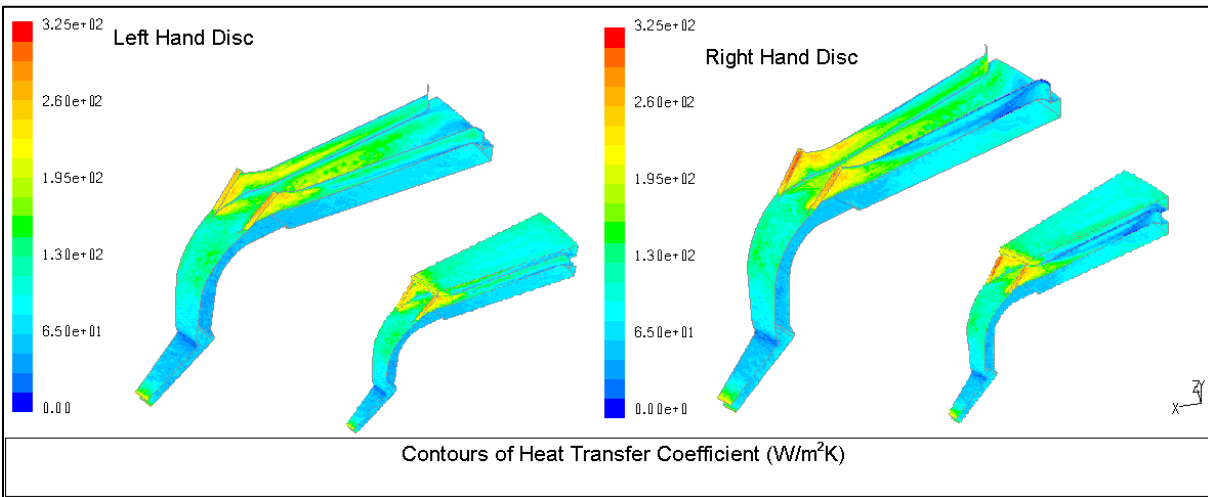


Figure 7: Local Heat Transfer Coefficient